SiO2 Reinforced HDPE Hybrid Materials Obtained by the Sol–Gel Method

Wenzhong Ma, Fanghong Gong, Chunlin Liu, Guoliang Tao, Jianping Xu, Bibiao Jiang

College of Materials Science and Engineering, Changzhou University, Changzhou 213164, China
Correspondence to: F. Gong (E-mail: fhgong@ccuz.edu.cn)

ABSTRACT: Novel high density polyethylene (HDPE)/SiO2 hybrid materials were prepared by the sol–gel process using tetraethoxysilane (TEOS). HDPE and synthesized HDPE-g-vinyl trimethoxysilane (VTMS) through melt grafting method was used as the raw material. The structure and thermal, mechanical properties of hybrid materials were investigated by Fourier transform infrared (FTIR) spectroscopy, X-ray photoelectron spectroscopy (XPS), scanning electron microscopy (SEM), simultaneous thermogravimetric (TG), differential thermal analysis (DTA), and tensile tests, respectively. Silica phase in the HDPE-g-VTMS hybrids showed a network structure and nano-scale size. The covalent bonds between organic and inorganic phases were introduced by the HDPE-g-VTMS bearing trimethoxysilyl groups, which underwent hydrolytic polycondensation with TEOS. The thermal stability and mechanical properties of HDPE-g-VTMS hybrids were obviously improved by embedded silica networks. It was found that the silica content in the HDPE-g-VTMS hybrid material was linearly increased with the TEOS dosage. The formation of the HDPE-g-VTMS hybrid was beneficial for enhanced mechanical strength and thermal stability, in comparison with the neat HDPE. © 2013 Wiley Periodicals, Inc. J. Appl. Polym. Sci. **2014**, *131*, 39891.

INTRODUCTION

The sol–gel (S-G) process for one of organic–inorganic hybrid material preparations has been of great interest in various fields, such as coatings techniques,[1] functional ceramic materials,[2] nanomaterials preparation,[3,4] and etc., since developed in the 1930s.[5] Thus, the preparation, characterization, and applications of organic/inorganic hybrid materials have become a fast expanding area of research in materials science, which is due to its new and different properties of the nanocomposites in comparison with the traditional composites.[6] For example, the tensile strength and Young's modulus of chitosan/graphene oxide (GO) nanocomposite were significantly improved by about 122% and 64%, respectively, in comparison with the pure chitosan.[7] For polymethyl methacrylate (PMMA)/mutiwalled carbon nanotubes (MWNTs) composite, the storage modulus was significantly enhanced by ~1100% as compared with commercial PMMA.[8] According to the possible interactions connecting the inorganic and organic species, it can be classified into weak interactions between the two phases (such as van der Waals, hydrogen bonding, or weak electrostatic interactions) and strong chemical interactions between the components such as covalent bonds.[9,10] Recently, the S-G process has been applied to produce organic/inorganic hybrid materials for many

polymers, such as PMMA,[11] polystyrene (PS),[12] polyimide,[13] poly(epsilon-caprolactone) (PCL),[14] polytrafluoroethylene (PTFE),[15] poly(vinyl alcohol) (PVA),[16] and so on.

Most of the research work about hybrid materials was focused on the nanoparticles dispersion in a polar polymer.[11–15,17] In order to improve the interfacial adhesion, the nanoparticle surface has to be modified, such as covering with a layer of a matri-miscible polymer,[18] immobilization of catalysts on nanoparticle surface,[19,20] and *in situ* nanoparticle synthesis[6] graft polymers can be used as compatibilizer, which can satisfy compatibility with the fillers. Since the number of polymers bearing functional groups that could form hydrogen bonds is rather limited, coupling agents are used to introduce covalent bonds between two phases. The most popular method of adding the coupling agents is accomplished by a reaction with the performed polymer to modify it.[10] As reported by Zhou et al.,[21] poly(styrene-co-maleic anhydride)/silica hybrid material has been successfully prepared from styrene–maleic anhydride copolymer and tetraethoxysilane (TEOS) in the presence of a coupling agent (3-aminopropyl) triethoxysilane (APTES) by an *in situ* S-G process. When polycondensation takes place between trialkoxysilyl groups on the polymer and TEOS, covalent bonds between two phases can be formed.

Table I. Sample Lists of Prepared HDPE/SiO$_2$ Hybrid Materials

Sample	HDPE-g-VTMS (wt %)	HDPE (wt %)	TEOS (wt %)	H$_2$O (wt %)	SiO$_2$[a] (wt %)
HDPE-g-VTMS	100	0	0	0	0
HDPE/SiO$_2$	0	98.7	1.0	0.3	0.30
HDPE-g-VTMS/SiO$_2$-1	98.7	0	1.0	0.3	0.50
HDPE-g-VTMS/SiO$_2$-2	98.0	0	1.5	0.5	0.72
HDPE-g-VTMS/SiO$_2$-3	97.3	0	2.0	0.7	0.91
HDPE-g-VTMS/SiO$_2$-4	96.7	0	2.5	0.8	1.20
HDPE-g-VTMS/SiO$_2$-5	96.0	0	3.0	1.0	1.52

[a] Calculated SiO$_2$ content (wt %) in the hybrid material was based on the mass ratio of ash SiO$_2$ and hybrid material.

As for the preparation of polyethylene (PE) hybrids, the achievable maximum volume fractions without aggregation are limited. Recently, completely miscible PE nanocomposites was established based on polymer-brush-coated nanoparticles.[18] However, the PE-coated nanoparticles were difficult to synthesize. In our previous work,[22] the vinyl trimethoxy silane (VTMS) can be successfully grafted to the PE molecular chain, resulting in the silane-grafted PE. The modification of PE polymer is also effective for controlling morphology and achieving a good adhesion between organic and inorganic phases. Melt processing has been can chosen because it is a cost-effective and environment friendly method, which avoids the use of any solvent. The purpose of this study is to synthesize and characterize the structure and properties of HDPE/silica hybrid materials manufactured via two different processes: synthesis of the HDPE-g-vinyl trimethoxysilane (VTMS) through melt grafting method and formation of silica phase in HDPE-g-VTMS phase. The relationship between the morphology, thermal stability, and mechanical properties and cooperation of the SiO$_2$ phase to the HDPE-g-VTMS phase was clarified. The prepared hybrid materials in this work can be expected to have potential applications in high performance membrane preparation.

EXPERIMENTAL

Materials

Commercial high density polyethylene (HDPE, 6070) was purchased from PetroChina Dushanzi Petrochemical Company, China. Acetone AR was purchased from Sinopharm group Co., Led., China. VTMS (A171) was purchased from Wuhan Tian Mu Technology Co., Ltd., China. TEOS and hydrochloric acid (HCl) were purchased from Changzhou Chemical Reagent, China. Dicumyl peroxide (DCP) was purchased from Tianjin Chemical Reagent, China. Antioxidant (1010) was purchased from Wunjin Chemical Reagent, China. VTMS, TEOS, DCP, and antioxidant were industrial products. These agents were used without any purification.

Melt Grafting of VTMS onto HDPE

The powders of HDPE/VTMS/DCP/antioxidant were mixed with a mass ratio of 100/1.6/0.08/0.2 in the twin-screw extruder (TE-34, Nanjing KY Chemical Machinery Co., Let., China). The reaction of melt grafting was proceeded during the melt extrusion process. The rate of screw was 160 r/min, the processing temperature of the extruder was set at 130, 150, 170, 190, 200,

and 190°C from the hopper to the die. After the melt extrusion process, the pellets of graft HDPE (HDPE-g-VTMS) was obtained by a granulator. As reported in our previous work, 1.6 wt % of VTMS was applied because of the highest grafting efficiency in this condition,[22] so we prepared HDPE-g-VTMS/SiO$_2$ hybrid material based on HDPE-g-VTMS with 1.6 wt % of VTMS addition in the following work.

Preparation of HDPE-g-VTMS/SiO$_2$ Hybrid Material

For the HDPE-g-VTMS/SiO$_2$ hybrid materials, the melt processing was used. TEOS was used to make SiO$_2$. Adequate contents of HCl and deionized water were introduced as a catalyst and a hydrolysis reagent, respectively. First, the HDPE-g-VTMS and TEOS were mixed in the internal mixer (S(X)M-1L-KA, Changzhou Suyuan Rubber Technology Co., Led., China) at 160°C. After melting for 5 min, adequate contents of HCl and deionized water were added (HCl/H$_2$O = 0.05/1 wt/wt), followed by the S-G reaction. This reaction was stopped until the torque reached an equilibrium state in the sample. After TEOS was completely hydrolyzed and condensed, a HDPE-g-VTMS/SiO$_2$ hybrid material was obtained. A neat HDPE/SiO$_2$ hybrid material was also prepared for the comparison of some properties of the HDPE-g-VTMS/SiO$_2$ hybrid material (with 1.0 wt % TEOS addition). Samples prepared in this way are summarized in Table I.

Experimental Techniques

In order to remove the unreacted VMTS monomer in HDPE-g-VTMS, HDPE-g-VTMS was dissolved into floccules by xylene, and then the floccule was extracted by acetone for 6 h. After extraction, HDPE-g-VTMS was dried in a vacuum oven for 5 h at 60°C. Thus, the dried HDPE-g-VTMS was used for measurements.

Infrared (IR) spectra were recorded with a Shimadzu IR-460 Fourier transform infrared (FTIR) spectrometer. One hundred scans at a resolution of 4 cm^{-1} were averaged to obtain each spectrum. X-ray photoelectron spectroscopy (XPS) was performed using Mg Kα radiation from a PHI5300x (Perkin–Elmer, USA) X-ray photoelectron spectrometer. Scanning electron microscopy (SEM) photographs were taken on a Jeol (Jeol, Japan) JSM-6360LA scanning electron microscope. Simultaneous thermogravimetric (TG) and differential thermal analysis (DTA) measurements (Diamond TG/DTA, Perkin Elmer, American) were carried out on the neat HDPE, HDPE-g-VTMS/SiO$_2$
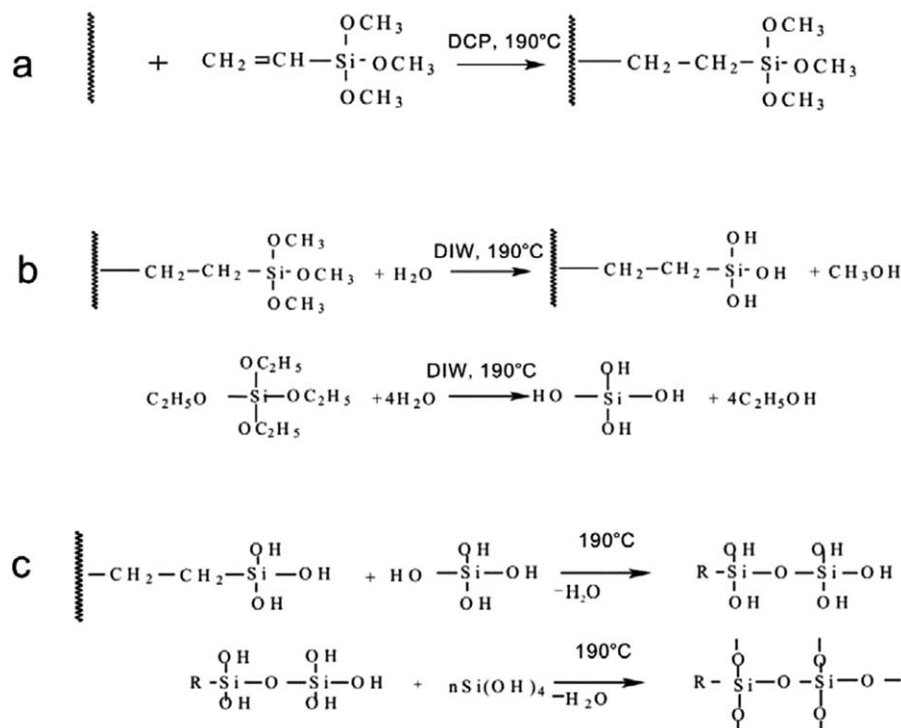
Scheme 1. Synthesis of HDPE-*g*-VTMS and its hybrid material by sol–gel process ("R" represents the C—C bonds in the HDPE-*g*-VTMS sample).

hybrid materials at a rate of 20 °C/min from room temperature to 200°C and up to 500°C at a rate of 5 °C/min. The sample was heated under N_2 atmosphere. The derivative thermogravimetry (DTA) curves and decomposition temperatures were obtained. Mechanical properties were determined by a testing machine (Shanghai, China). The specimens for tensile tests were dumbbell shaped cut from the molded polymer samples according to GB1040-92 (ISO604-1973) and carried out at a crosshead speed of 50 mm/min and 23 ± 2 °C. A 25 mm benchmark and the original cross-sectional area were utilized to calculate their tensile properties. Transmission electron microscopy (TEM) was carried out with JEOL-Z100 apparatus. Before the observation, the ultrathin slice samples were prepared.

RESULTS AND DISCUSSION

HDPE-*g*-VTMS/SiO$_2$ Hybrid Mechanism

As shown in Scheme 1, the synthesis of a typical HDPE/SiO$_2$ hybrid material includes three steps: (1) melt grafting of VTMS onto HDPE (Reaction a); (2) the preparation of silica by hydrolysis and condensation of TEOS in HDPE-*g*-VTMS (Reaction b); (3) the reaction between silica and HDPE-*g*-VTMS (Reaction c). Finally, HDPE-*g*-VTMS/SiO$_2$ hybrid material was obtained.

In this process, the sol evolves gradually toward the formation of a gel-like network, in which typical precursors (TEOS) undergo hydrolysis and polycondensation reactions to form a colloid. These hybrids are composites consisting of two constituents at the nanometer or molecular level. In most cases, the inorganic part in hybrid materials provides mechanical strength, while the organic part delivers linking between the inorganic phases.

FTIR Analysis of HDPE-*g*-VTMS and its Hybrid Material

With DCP as catalyst and in the presence of antioxidant, HDPE-*g*-VTMS was synthesized by melt grafting method. Identification of VTMS grafting to HDPE in this work was carried out with IR spectroscopy (Figure 1). As demonstrated in our previous work,[22] VTMS can be copolymerized to form HDPE-*g*-VTMS. So, compared with the HDPE sample, HDPE-*g*-VTMS displays an apparent Si—O—C with absorption peaks at 790 and 1100 cm^{-1}.[23]

The hybrid material HDPE-*g*-VTMS/SiO$_2$ (1.0 wt% TEOS) prepared through hydrolysis and polycondensation with TEOS forms absorption peaks at 1167 and 1080 cm^{-1}, representing
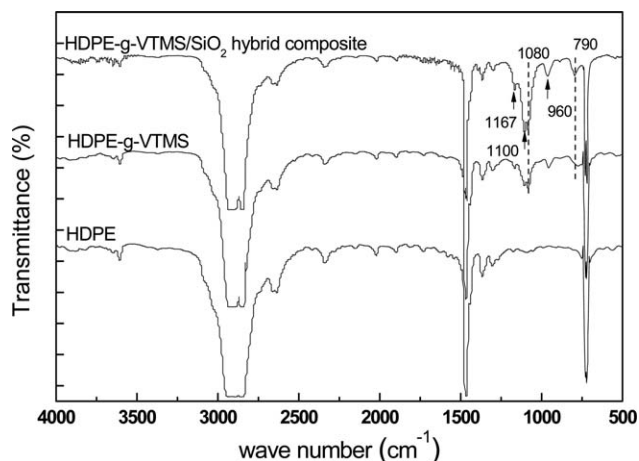

Figure 1. FTIR spectra of HDPE, HEPE-*g*-VTMS, and HDPE-*g*-VTMS/SiO$_2$ (1.0 wt % TEOS) hybrid material.

Si—O—Si asymmetric stretching. The hybrid material also has an absorption peak at 960 cm^{-1}, which refers to the Si—OH symmetric stretching.[23,24] The absorption peak of the Si—O—Si indicates a formation of the hybrid material HDPE-*g*-VEMS/SiO$_2$. On comparison of hybrid material and HDPE-*g*-VTMS, small absorption peaks of Si—O—Si in the hybrid material (indicated by the arrows) are still observed. This may be due to the moisture in the air, leading to a small amount of hydrolysis and polycondensation of HDPE-*g*-VTMS.

XPS Analysis of HDPE-*g*-VTMS and its Hybrid Material

Figure 2 illustrates the XPS spectrum of HDPE/SiO$_2$ hybrid materials. For HDPE/SiO$_2$ and HDPE-*g*-VTMS/SiO$_2$ hybrid material, the peak Si2p is at 101.9 eV and 103.0 eV, respectively. Peak Si2p for HDPE-*g*-VTMS/SiO$_2$ hybrid material is 1.1 eV higher than that for HDPE/SiO$_2$ hybrid material. This implies that the hydroxyl groups of the silica sol derived from partial hydrolysis of TEOS can react with the hydroxyl groups of the silica sol derived from HDPE-*g*-VTMS and formed HDPE-*g*-VTMS/SiO$_2$ hybrid material. This fact agrees well with the conclusions drawn from FTIR analysis.

Morphologies of HDPE-*g*-VTMS/SiO$_2$ Hybrid Material

To investigate the dispersion of SiO$_2$ in the hybrid materials, we investigated the morphologies of HDPE-*g*-VTMS [Figure 3(a)], HDPE/SiO$_2$ hybrid material for 1.0 wt % TEOS [Figure 3(b)], and HDPE-*g*-VTMS/SiO$_2$ hybrid material for 1.0 wt % TEOS [Figure 3(c)]. In HDPE-*g*-VTMS, a dense structure with silica networks embedded in the cross-section is observed. The roughened texture is considered to be resulting from the melt grafting of VTMS onto HDPE (Scheme 1, Reaction a), and the small
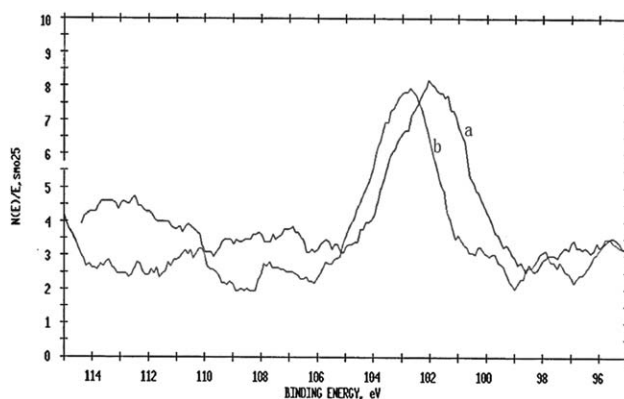

Figure 2. XPS spectrum of hybrid materials: (a) HDPE/SiO$_2$ hybrid material for 1.0 wt % TEOS; (b) HDPE-*g*-VTMS/SiO$_2$ hybrid material for 1.0 wt % TEOS.

voids could be attributed to the small amount of hydrolysis and polycondensation of HDPE-*g*-VTMS during the melt grafting process. This agrees with the result discussed in FTIR analysis. As shown in Figure 3, the cross-sectional structure of HDPE/SiO$_2$ and HDPE-*g*-VTMS/SiO$_2$ hybrid material illustrates a porous structure consisting of interconnected pores intertwining within the framework of the HDPE matrix. Based on these morphological characteristics and referring to the reactions shown in Scheme 1, it can be deduced that the pores in Figure 3 were produced by a mechanism associated with the hydrolysis and polycondensation of HDPE-*g*-VTMS during the melt grafting process (190°C). The gas produced from polycondensation expands at elevated temperature to generate pores in the HDPE
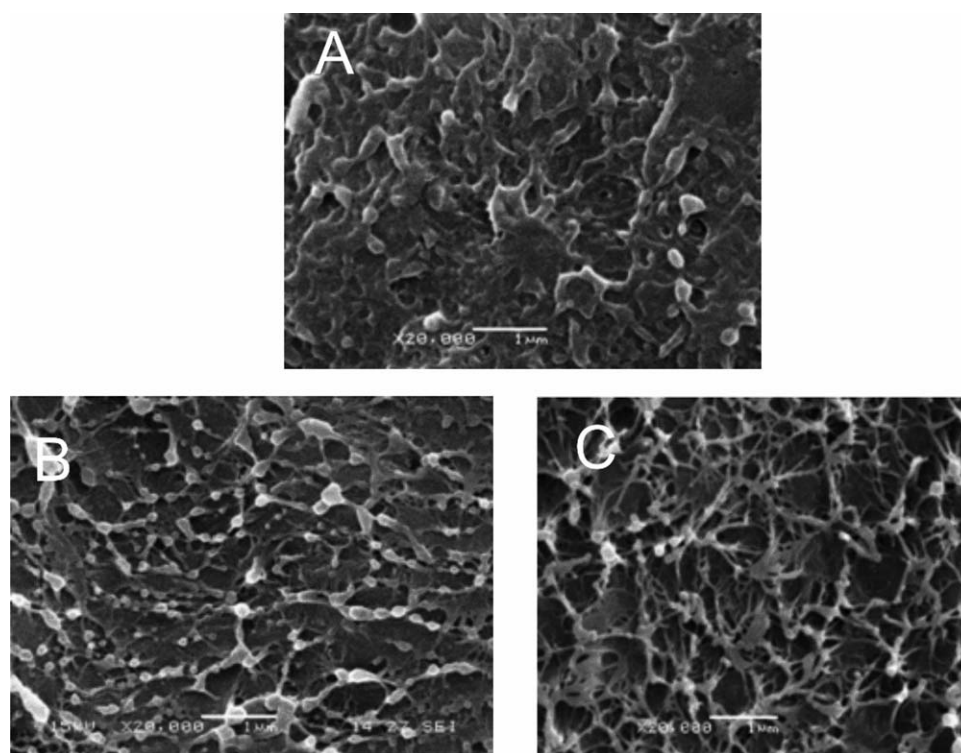

Figure 3. SEM photographs for hybrid materials: (A) HDPE-*g*-VTMS; (B) HDPE/SiO$_2$ hybrid material for 1.0 wt % TEOS; (C) HDPE-*g*-VTMS/SiO$_2$ hybrid material for 1.0 wt % TEOS.
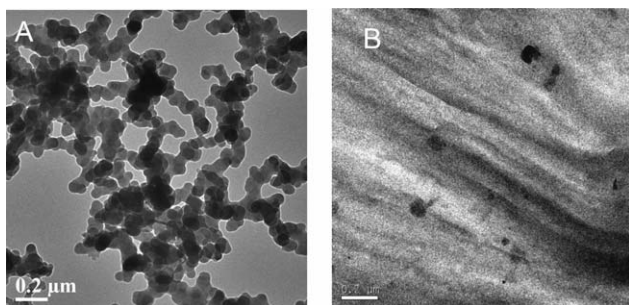
Figure 4. TEM micrographs of HDPE/SiO$_2$ hybrid material for 1.0 wt % TEOS (A), HDPE-*g*-VTMS/SiO$_2$ hybrid material for 1.0 wt % TEOS (B).

matrix. Compared with the neat HDPE/SiO$_2$ hybrid material, larger pores and smaller silica particles (around 100 nm) dispersed in the HDPE-*g*-VTMS/SiO$_2$ hybrid material are observed, which is due to the deeper hydrolysis and polycondensation of HDPE-*g*-VTMS during the melt extrusion process. As described in Scheme 1, the formation of HDPE-*g*-VTMS/SiO$_2$ hybrid material not only includes the hydrolysis and polycondensation of TEOS, but also contains the polycondensation between Si—OH in HDPE-*g*-VTMS and Si—OH in TEOS. The extensive hydrolysis and polycondensation in HDPE-*g*-VTMS/SiO$_2$ hybrid material leads to the larger pores in the hybrid material. Furthermore, due to the side chains Si—OCH$_3$ in HDPE-*g*-VTMS, TEOS undergoes polycondensation in these points, resulting in the formation of chemical bond between nano-scale SiO$_2$ and HDPE chains. Therefore, the nano-scaled SiO$_2$ dispersed in HDPE-*g*-VTMS/SiO$_2$ hybrid material.

In order to examine the phase morphology development of composites based on HDPE, TEM observation was carried out. The TEM images of HDPE/SiO$_2$ hybrid material for 1.0 wt % TEOS and HDPE-*g*-VTMS/SiO$_2$ hybrid material for 1.0 wt % TEOS are shown in Figure 4. In the TEM micrographs, the dark domains represent the silicate layers in the polymer matrix. A micro-scale dispersion of primary particles aggregates is observed in HDPE/SiO$_2$ hybrid material, leading to a high interfacial tension between the hydrophobic polymer (HDPE) and the hydrophilic SiO$_2$. In contrast, HDPE-*g*-VTMS/SiO$_2$ hybrid material exhibits a very fine dispersion of nearly nano-scaled SiO$_2$. This confirms the formation of chemical bond between SiO$_2$ and HDPE chains.

The Effect of TEOS Dosage on the SiO$_2$ Content in the HDPE-*g*-VTMS/SiO$_2$ Matrix

In order to obtain the ultimate SiO$_2$ content in the hybrid material, the TG/DTA technique was carried out on the HDPE-*g*-VTMS/SiO$_2$ hybrid materials with various TEOS dosage under N$_2$ atmosphere. Figure 5 shows the relationship between SiO$_2$ content in HDPE-*g*-VTMS/SiO$_2$ hybrid materials and the amount of TEOS dosage. The SiO$_2$ content in the HDPE-*g*-VTMS/SiO$_2$ matrix is linearly increased with an increase of TEOS dosage, which indicates that as more TEOS dosage applied, more SiO$_2$ content can be obtained. According to the linear trace in Figure 5 (as noted by the dashed line), when no TEOS is employed, about 0.4 wt % SiO$_2$ content is still in the HDPE-*g*-VTMS sample. This non-zero of SiO$_2$ content can be attributed to the hydrolysis and polycondensation of VTMS
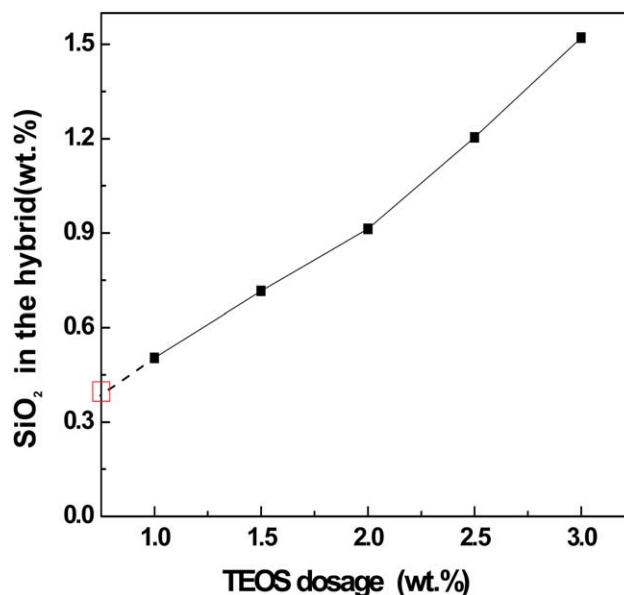

Figure 5. Relationship between SiO$_2$ content in HDPE-*g*-VTMS/SiO$_2$ hybrid materials and the amount of TEOS dosage. [Color figure can be viewed in the online issue, which is available at wileyonlinelibrary.com.]

grafting onto HDPE. This in turn verifies the results of FTIR and XPS analysis.

The Effect of Silica Content on the Thermal Stability of HDPE-*g*-VTMS/ SiO$_2$ Hybrid Material

Once new hybrids have been synthesized, knowledge of their decomposition characteristics is required. The amount of inorganic solids can be estimated from these TG curves. In this work, TG/DTA was carried out under N$_2$ atmosphere, so the inorganic solids can be considered as SiO$_2$. Figure 6 shows the
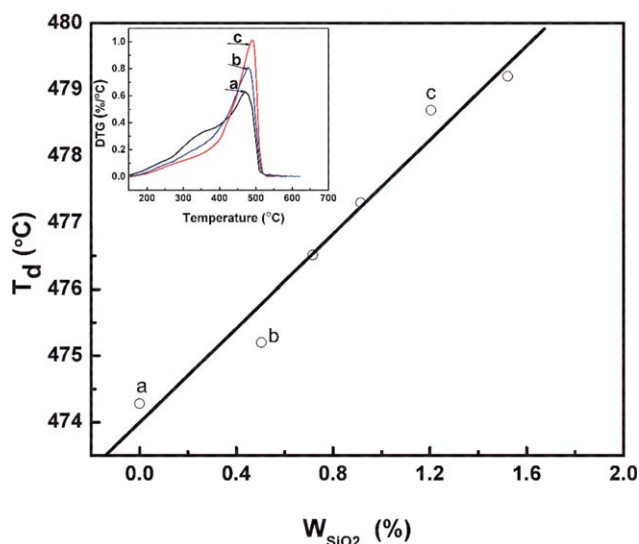

Figure 6. Influence of the SiO$_2$ content on the decomposition temperature (T_d) of HDPE-*g*-VTMS/SiO$_2$ hybrid materials. Upper left inset is the DTG curves referred to samples with different SiO$_2$ content: (a) neat HDPE, (b) 0.5 wt % SiO$_2$, (c) 1.2 wt % SiO$_2$. [Color figure can be viewed in the online issue, which is available at wileyonlinelibrary.com.]
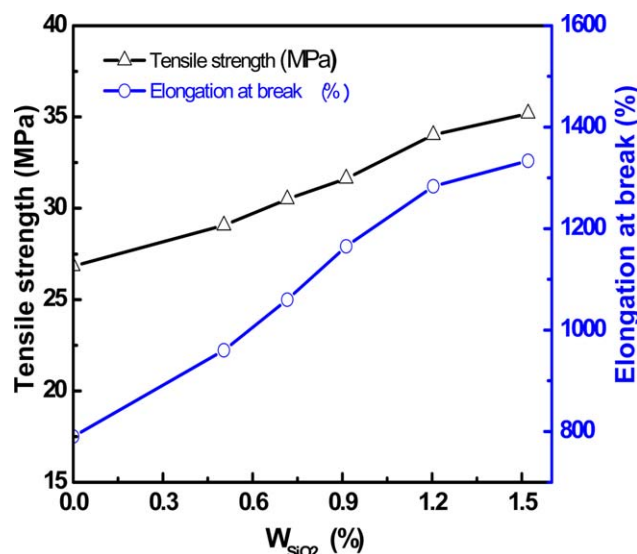
Figure 7. Dependence of tensile strength and elongation at break on the SiO_2 content for HDPE-*g*-VTMS/SiO_2 hybrid materials. [Color figure can be viewed in the online issue, which is available at wileyonlinelibrary.com.]

influence of the SiO_2 content on the decomposition temperature (T_d) of the HDPE-*g*-VTMS/SiO_2 hybrid materials. As the need for comparison, the neat HDPE was added into the test group. With an increase of SiO_2 in the hybrid material, T_d is increased, which suggests the improved thermal stability by the SiO_2 presence.[25] When the SiO_2 content increases up to 1.5 wt %, T_d is improved a little because of approaching the saturated amount of SiO_2.[26]

Under N_2 condition, a unique primary state of decomposition is observed in the neat HDPE and HDPE-*g*-VTMS/SiO_2 hybrid materials in the temperature range from 200 to 530°C, as represented in the upper inset of the left plot. The neat HDPE is completely decomposed at 510°C. The HDPE-*g*-VTMS/SiO_2 hybrid material, HDPE has a first weight change at around 300°C and begins the primary decomposition at 400°C (like other two hybrid materials). However, for HDPE-*g*-VTMS/SiO_2 hybrid materials this first decomposition at 300°C is not observed, which means that the presence of SiO_2 hinders the decomposition at high temperatures.

The Effect of Silica Content on the Mechanical Properties of HDPE-*g*-VTMS/SiO_2 Hybrid Material

Figure 7 represents the variations in the mechanical properties of HDPE-*g*-VTMS/SiO_2 hybrid materials with various SiO_2 contents. It can be seen from Figure 7 that the tensile strength and elongation at break are directly proportional to the SiO_2 content when the SiO_2 content is in the range of 0–1.5 wt %. The tensile strength and elongation at break of the hybrid materials with 1.5 wt % increased by 31% and 69%, respectively as compared to neat HDPE. This increase in mechanical properties stemmed from the restricted mobility of the polymer chains due to the efficient connection between the HDPE-*g*-VTMS and the SiO_2 nano-dispersed in the hybrid. In this work, the VTMS was firstly grafted to HDPE chains by melt grafting method, so this grafted chains can hydrolyze and polycondense with TEOS

[Scheme 1(b,c)], indicating the covalent bond formation between HDPE and SiO_2. As suggested by molecular-dynamics studies, the improved mechanical strength for nanocomposites is due to the ability of nanoparticles to dissipate energy.[27] Because of the comparable time scales for motion for nanoparticles and polymer chains, the nanoparticles can act as temporary crosslinks between polymer chains, providing localized regions of enhanced strength, which in turn can prevent destructive deformation.[28] It was reported that the tensile strength of ultrahigh molecular weight polyethylene (UHMWPE) ranges from 36 to 46 MPa.[29] Hence, it is concluded that the present HDPE hybrid material has comparative mechanical strength as that of UHMWPE.

CONCLUSIONS

In this study, we examined the preparation of high performance HDPE hybrid through the S-G process using TEOS and synthesized HDPE-*g*-VTMS containing 1.6 wt % of VTMS as raw material. FTIR and XPS analysis verified that VTMS was successfully copolymerized to form HDPE-*g*-VTMS by melt grafting method. HDPE-*g*-VTMS and silica units were linked by covalent bonds in HDPE-*g*-VTMS hybrids. As illustrated from the cross-sectional structure, silica phase in the HDPE-*g*-VTMS hybrids showed a network structure and nano-scale size, which led to much better thermal stability and mechanical properties compared to that of the neat HDPE. The silica content in the HDPE-*g*-VTMS hybrid material was linearly increased with the TEOS dosage. Furthermore, the decomposition temperature and tensile strength were linearly increased with an increase in silica content in the hybrids.

REFERENCES

1. Troczynski, T.; Liu, D. M. U.S. Pat. 6,426,114 (**2002**).

2. Chen, Q.; Soutar, A. M. *Key Eng. Mater.* **2009**, *391*, 79.

3. Oskam, G.; Poot, F. J. P. *J. Sol-Gel Sci. Technol.* **2006**, *37*, 157.

4. Badheka, R.; Johnson, A.; Perry, C. C.; Sermon, P. A.; Taylor, A.; Vong, M. S. W. *J. Mater. Chem.* **2002**, *12*, 3278.

5. Noell, J. L. W.; Wilkes, G. L.; Mohanty, D. K.; McGrath, J. E. *J. Appl. Polym. Sci.* **1990**, *40*, 1177.

6. Zhu, J.; Wei, S.; Li, Y.; Sun, L.; Haldolaarachchige, N.; Young, D. P.; Southworth, C.; Khasanov, A.; Luo, Z.; Guo, Z. *Macromolecules* **2011**, *44*, 4382.

7. Yang, X.; Tu, Y.; Li, L.; Shang, S.; Tao, X. *Appl. Mater. Interfaces* **2010**, *6*, 1707.

8. Hwang, G. L.; Shieh, Y. T.; Hwang, K. C. *Adv. Funct. Mater.* **2004**, *5*, 487.

9. Wen, J.; Wilkes, G. L. *Chem. Mater.* **1996**, *8*, 1667.

10. Zou, H.; Wu, S.; Shen, J. *Chem. Rev.* **2008**, *108*, 3893.

11. Lee, L. H.; Chen, W. C. *Chem. Mater.* **2001**, *13*, 1137.

12. Tamaki, R.; Chujo, Y. *J. Mater. Chem.* **1998**, *8*, 1113.

13. Schramm, C.; Rinderer, B.; Tessadri, R. *J. Appl. Polym. Sci.* **2013**, *128*, 1274.

14. Machado, A. V.; Amorim, S.; Botelho, G.; Neves, I. C.; Fonseca, A. M. *J. Mater. Sci.* **2013**, *48*, 3578.

15. Zhang, D. N.; Kou, K. C.; Gao, P.; Hou, M.; Chao, M. *J. Polym. Res.* **2012**, *19*, 1.

16. Kuraoka, K.; Hashimoto, A. *J. Ceram. Soc. Jpn.* **2008**, *116*, 832.

17. Haraguchi, K.; Usami, Y.; Ono, Y. *J. Mater. Sci.* **1998**, *33*, 3337.

18. Bieligmeyer, M.; Taheri, S. M.; German, I.; Boisson, C.; Probst, C.; Milius, W.; Altstadt, V.; Breu, J.; Schmidt, H. W.; D'Agosto, F.; Forster, S. *J. Am. Chem. Soc.* **2012**, *134*, 18157.

19. Fischer, S.; Salcher, A.; Kornowski, A.; Weller, H.; Förster, S. *Angew. Chem. Int. Ed.* **2011**, *50*, 7811.

20. Wang, T. L.; Ou, C. C.; Yang, C. H. *J. Appl. Polym. Sci.* **2008**, *109*, 3421.

21. Zhou, W.; Dong, J. H.; Qiu, K. Y.; Wei, Y. *J. Polym. Sci. Part A: Polym. Chem.* **1998**, *36*, 1607.

22. Gong, F. H.; Jiang, B. B.; Liu, C. L.; Wang, X.; Lu, L. D.; Yang, X. *J. Polym. Mater. Sci. Eng.* (China) **2006**, *22*, 173.

23. Yeh, J. T.; Chen, C. L.; Huang, K. S. *J. Appl. Polym. Sci.* **2007**, *103*, 1140.

24. Araki, W.; Adachi, T. *J. Appl. Polym. Sci.* **2008**, *107*, 253.

25. Xiong, M. N.; You, B.; Zhou, S. X.; Wu, L. M. *Polymer* **2004**, *45*, 2967.

26. Ma, W.; Wang, X.; Zhang, J. *J. Polym. Sci. Part B: Polym. Phys.* **2010**, *48*, 2154.

27. Gersappe, D. *Phys. Rev. Lett.* **2002**, *89*, 058301.

28. Shah, D.; Maiti, P.; Gunn, E.; Schmidt, D. F.; Jiang, D. D.; Batt, C. A.; Giannelis, E. P. *Adv. Mater.* **2004**, *16*, 1173.

29. Fouad, H. *Mater. Design.* **2010**, *31*, 1117.